Biomedicine & Pharmacotherapy 170 (2024) 116032

Contents lists available at ScienceDirect

Biomedicine & Pharmacotherapy

journal homepage: www.elsevier.com/locate/biopha

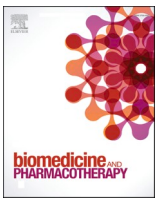

CCBE1 regulates the development and prevents the age-dependent regression of meningeal lymphatics

Zsombor Ocskay [a], László Bálint [a], Carolin Christ [a], Mark L. Kahn [b], Zoltán Jakus [a,*]

[a] Department of Physiology, Semmelweis University School of Medicine, Budapest, Hungary
[b] Cardiovascular Institute, Department of Medicine, Perelman School of Medicine, University of Pennsylvania, Philadelphia, Pennsylvania, PA, USA

ARTICLE INFO

Keywords:
Meningeal lymphatics
CCBE1
Lymphatic development
Aging
Lymphatic maintenance

ABSTRACT

Recent studies have described the importance of lymphatics in numerous organ-specific physiological and pathological processes. The role of meningeal lymphatics in various neurological and cerebrovascular diseases has been suggested. It has also been shown that these structures develop postnatally and are altered by aging and that the vascular endothelial growth factor C (VEGFC)/ vascular endothelial growth factor receptor 3 (VEGFR3) signaling plays an essential role in the development and maintenance of them. However, the molecular mechanisms governing the development and maintenance of meningeal lymphatics are still poorly characterized. Recent in vitro cell culture-based experiments, and in vivo studies in zebrafish and mouse skin suggest that collagen and calcium binding EGF domains 1 (CCBE1) is involved in the processing of VEGFC. However, the organ-specific role of CCBE1 in developmental lymphangiogenesis and maintenance of lymphatics remains unclear. Here, we aimed to investigate the organ-specific functions of CCBE1 in developmental lymphangiogenesis and maintenance of meningeal lymphatics during aging. We demonstrate that inducible deletion of CCBE1 leads to impaired postnatal development of the meningeal lymphatics and decreased macromolecule drainage to deep cervical lymph nodes. The structural integrity and density of meningeal lymphatics are gradually altered during aging. Furthermore, the meningeal lymphatic structures in adults showed regression after inducible CCBE1 deletion. Collectively, our results indicate the importance of CCBE1-dependent mechanisms not only in the development, but also in the prevention of the age-related regression of meningeal lymphatics. Therefore, targeting CCBE1 may be a good therapeutic strategy to prevent age-related degeneration of meningeal lymphatics.

1. Introduction

Lymphatics play an essential role in maintaining fluid homeostasis by facilitating the drainage of interstitial fluid and macromolecules, providing immune surveillance by transporting immune cells and soluble antigens, and mediating the absorption and transport of dietary lipids from the small intestine [1,2]. A vast amount of recent experimental data indicates that the lymphatic system has several novel and unexpected physiological and pathophysiological functions, including a role in obesity, cardiac regeneration, hypertension, postnatal pulmonary adaptation and meningeal lymphatics mediated clearance of macromolecules from the central nervous system (CNS) [1–4]. Most of these functions show organ- and tissue-specific characteristics, highlighting the importance of understanding the organ-specific functions of lymphatics.

Vascular endothelial growth factor C (VEGFC) is the most important known lymphangiogenic factor [1,2]. Lack of VEGFC leads to the abrogation of lymphatic development [5]. It has also been described that proteolytic cleavage of VEGFC is required to generate the mature form, which mediates the stimulation of lymphatic growth and function through vascular endothelial growth factor receptor-3 (VEGFR3) signaling [6–8]. Loss of function mutations in the gene *FLT4*, encoding VEGFR3, reportedly disrupt the VEGFC/VEGFR3 signaling axis, and thereby are responsible for the pathophysiology of Milroy's disease, a

Abbreviations: ADAMTS3, A disintegrin and metalloproteinase with thrombospondin motifs 3; CCBE1, Collagen and calcium binding EGF domains 1; CNS, Central nervous system; FLT4, Fms related receptor tyrosine kinase 4; GFP, Green fluorescent protein; KLK3, Kallikrein related peptidase 3; LV, Lymphatic vessel; LYVE1, Lymphatic vessel endothelial hyaluronan receptor 1; P, Postnatal day; PBS, Phosphate-buffered saline; PDPN, Podoplanin; PFA, Paraformaldehyde; RhD, Rhodamine dextran; VEGFC, Vascular endothelial growth factor C; VEGFR3, Vascular endothelial growth factor receptor 3; VWF, Von Willebrand factor.

* Correspondence to: Semmelweis University School of Medicine, Department of Physiology, Tűzoltó utca 37-47, 1094 Budapest, Hungary.
E-mail address: jakus.zoltan@med.semmelweis-univ.hu (Z. Jakus).

https://doi.org/10.1016/j.biopha.2023.116032
Received 26 July 2023; Received in revised form 12 December 2023; Accepted 14 December 2023
Available online 22 December 2023

typical form of primary lymphedema. [9].

Primary lymphedema is also the leading symptom in Hennekam syndrome, a condition additionally associated with mental retardation and bone developmental defects [10]. Mutations of collagen and calcium binding EGF domains 1 (CCBE1) were identified to cause Hennekam syndrome in many affected patients in an autosomal recessive manner [11,12]. Further investigation of CCBE1 revealed its important role in embryonic lymphangiogenesis in zebrafish and mice [13–16]. Thereafter, in vitro studies using cell culture-based models and zebrafish experiments suggested that CCBE1 is involved in the processing of the full-length form of VEGFC [17,18]. After the harvesting from cell culture supernatants, A disintegrin and metalloproteinase with thrombospondin motifs-3 (ADAMTS3) protease was identified as a catalyst of VEGFC processing in cooperation with CCBE1 [17]. Thereafter, in vivo studies indicated the role of CCBE1 in the processing of VEGFC in the mouse skin to generate the active and mature form of the lymphangiogenic factor [19]. However, the organ-specific role of CCBE1 in lymphangiogenesis and maintenance of lymphatics remains unclear in other tissues and organs.

It is well established that lymphatics are present in the dura mater adjacent to the venous sinuses [3,4,20–22]. Meningeal lymphatic vessels were identified not only in mice but also in non-human primates and humans [23]. Studies in mouse models have suggested the possible role of meningeal lymphatic vessels in various neurological diseases affecting the CNS, such as Alzheimer's disease, multiple sclerosis and autoimmune encephalitis [21,22,24–27]. These findings indicate that meningeal lymphatic vessels, which develop postnatally, play an essential role in maintaining physiological functions of the CNS and their possible involvement in various pathophysiological processes [3, 20,21,28]. The morphology and function of meningeal lymphatic vessels in mice have been observed to be impaired by aging [4,28]. A similar age-dependent decrease in the function of meningeal lymphatic vessels was found in aged humans [29]. The VEGFC/VEGFR3 signaling axis is essential for their development and maintenance [30]. However, the potential role of other regulators of the developmental program and maintenance of meningeal lymphatic vessels, such as CCBE1, remains unclear.

Here, we aimed to characterize the age-dependent changes of meningeal lymphatic vessels and the role of CCBE1 in the developmental program and maintenance of these vessels, using a conditional knockout mouse strain, which enables for the induced deletion of CCBE1 in vivo. Our findings demonstrate a CCBE1-dependent mechanism in the development and the prevention of age-related regression of meningeal lymphatic vessels. Our results suggest that targeting CCBE1 may be a good therapeutic strategy to prevent age-related regression of meningeal lymphatic vessels.

2. Materials and methods

2.1. Animals

Newborn, adult (1–6 months), middle-aged (10–14 months) and old (older than 18 months) C57BL/6 wild type and *Prox1*^{GFP} lymphatic reporter mice were used to visualize lymphatic vasculature [31]. *Prox1*^{GFP} mice were maintained in heterozygous form and genotyped by a transgene specific PCR using 5′ - GAT GTG CCA TAA ATC CCA GAG CCT AT – 3′forward and 5′ - GGT CGG GGT AGC GGC TGA A - 3′ reverse primers. To characterize the expression pattern of CCBE1 in the dura mater we used 7-and 15-day-old (P7 and P15) *Ccbe1*$^{LacZ/+}$ and littermate control mice (note that the *Ccbe1*^{LacZ} reporter allele is a null *Ccbe1*$^{-}$ allele) [15, 32]. To investigate the possible role of CCBE1 in the organ-specific lymphatic development and maintenance, we used newborn and adult (1–6 months) Ub-CreER^{T2}; *Ccbe1*$^{fl/-}$ and littermate control mice [15,19, 32]. The strain was maintained in heterozygous form and allele-specific PCR was performed to genotype the Ub-CreER^{T2}, *Ccbe1*$^{fl/-}$ strain. The following primers were used: for the *Ccbe1* knockout allele, forward (5′ – TGG GAG TTG AAT CCC TGA TGG TCT – 3′) and reverse (5′ – AGG CCA TAC AAG TGT TGG GCA TTG – 3), for the *Ccbe1* wild type allele, specific forward (5′ – CAG AGC AAA GGG ACA ACA GGT G – 3′) and reverse (5′ – TAA ACA CGG CAG CAG CAA CC – 3′), for the *Ccbe1* conditional allele, forward (5′ – GGG GTC CAT GCT TAG CAA GC – 3′) and reverse (5′ – TTT AGG GCT AGG CTG TGT AAT TGG – 3′), and for Ub-Cre, forward (5′ – GCG GTC TGG CAG TAA AAA CTA TC – 3′) and reverse (5′ – GTG AAA CAG CAT TGC TGT CAC TT – 3′) primers. Mice of all strains were kept in an environment with controlled temperature and humidity, on 12 h light/dark cycles. Experimental animals were housed in either specific pathogen free or conventional animal facilities.

2.2. Induction of Cre-mediated Ccbe1 deletion

To induce the Cre-mediated deletion of *Ccbe1* in newborn mice, the newborns were injected with intragastrical Tamoxifen (Sigma-Aldrich, St. Louis, USA) (50 μL 2 mg/ml Tamoxifen dissolved in ethanol/ corn oil) on day 1 after birth (P1). In adult mice, deletion of *Ccbe1* was induced in 2-month-old mice by a 3 week-long Tamoxifen diet as described previously [19].

2.3. Isolation of meninges

To study the structural characteristics of meningeal lymphatics during development and aging, we isolated meninges of newborn (5 days old), adult (1–6 months old), middle-aged (10–14 months old) and old (18 or more months old) mice. Our isolation protocol was based on the protocol of Louveau and Kipnis as described previously [20,33]. Mice were transcardially perfused with 10 ml phosphate-buffered saline (PBS) followed by 10 ml of 4% paraformaldehyde (PFA) (Sigma-Aldrich, St. Louis, USA). Using scissors and forceps, skin and muscles were removed from the skull followed by the dissection of optic nerves, eyeballs and mandibles. After removal of the lower orbits and nasal bone, the basal portion of the skull was cut and separated. After the skull was separated, the brain was scooped out of the dorsal half of the skull. Meninges attached to the skull were then fixed in 4% PFA overnight at 4 °C and washed with PBS.

2.4. Whole-Mount Immunostaining

Isolated meninges and ears were incubated for 1 h in PBS containing 10% goat or horse serum at room temperature, followed by staining with antibodies for LYVE-1 (R&D Systems, AF2125, Minneapolis, USA), PDPN (BioLegend, 127402, San Diego, USA), VWF (Thermo Fisher Scientific, PA5–16634, Waltham, USA), GFP (Life Technologies, A11122, Waltham, USA) as described previously [33]. All primary antibodies were diluted 1:170 in the presence of 10% serum and 0.1% Tween 20 (Sigma-Aldrich, St. Louis, USA) and incubated for 24 h at 4 °C. Thereafter, samples were incubated for 1 h with Alexa Fluor 488/568/594 anti-rabbit/anti-goat/anti-Syrian hamster IgG antibodies (Life Technologies, A21206, A11055, A11057, A11006, A11077, A21113 at 1:1000, Waltham, USA) at room temperature in PBS containing 2% serum and 0.1% Tween 20. After the staining, tissues were washed with PBS. Control immunostaining of samples for all experiments has been performed.

2.5. β-galactosidase staining

CCBE1 reporter gene expression was investigated in wild type (*Ccbe1*$^{+/+}$) and *Ccbe1*$^{LacZ/+}$ mice at P7 and P15 using whole-mount samples for detecting β-galactosidase activity, based on the method-described by Puri et al. [34] further optimized for the staining of meninges. Skull samples with attached meninges were dissected in PBS and then fixed in 2% PFA for 30 min. Post-fixation, the samples were washed with PBS for 30 min at 4 °C. The samples were then stained in 25 mg/ml X-gal (Sigma-Aldrich, St. Louis, USA) (dissolved in

dimethylformamide (Acros Organics, Waltham, USA)), 2.5 mM $K_3[Fe(CN)_6]$ (Fisher Scientific, Waltham, USA), 2.5 mM $K_4[Fe(CN)_6]$ (Acros Organics, Waltham, USA), 5 mM $MgCl_2$ (Fisher Scientific, Waltham, USA) in PBS at 37 °C for 12–18 h. Following LacZ staining, samples were washed at room temperature for 30 min and then fixed in 2% PFA overnight. After the second fixation, samples were washed and stored in PBS, then examined with a stereomicroscope. Next, the samples were embedded in paraffin, sectioned and stained using antibodies against blood and lymphatic vessel markers as previously described [32,35].

2.6. Assessment of meningeal lymphatic function

To monitor meningeal lymphatic function, mice were anesthetized by an intraperitoneal injection of 2.5 % Avertin (Sigma-Aldrich, St. Louis, USA) followed by an injection of 2.5 μL of 70 kDa Rhodamine dextran (RhD) (Life Technologies, Waltham, USA) from a 10 mg/ml stock 2 mm deep into the dorsal prefrontal cortex of the right hemisphere or into the cisterna magna of mice. For intraparenchymal injection, a midline skin incision was made to reveal the skull bone, which was thinned 2 mm lateral and 1.5 mm caudal to the bregma. The tracer was slowly injected ~2 mm deep with a Hamilton syringe using a blunt-ended 30 G needle over 3 min. For intra-cisterna magna injections, the neck muscles were dissected through a small midline incision followed by injection of 70 kDa RhD into the cisterna magna with a Hamilton syringe using a sharp-ended 32 G needle over 3 min. After intraparenchymal or intra-cisterna magna injection, the needle was left in natural position, then it was slowly removed after 5 min to prevent leakage. All mice were sacrificed 100 min post-injection, and the appropriate injection location was confirmed. If the injection was unsuccessful, the mouse was excluded from the dataset. The uptake of fluorescently labeled macromolecules in the meningeal vessels or the deep cervical lymph nodes was investigated by fluorescence stereomicroscopy. Additionally, a lymphatic endothelial cell specific immunostaining was performed to visualize lymphatics. Drainage of the injected fluorescently labeled molecules into the cervical lymph nodes was quantified by measuring the mean fluorescence intensity of the area of the lymph nodes (mean fluorescent intensity of background subtracted from the mean fluorescence intensity of lymph nodes) using NIS-Elements Imaging Software (Nikon Instruments, Tokyo, Japan) as described previously [33].

2.7. Histological analyses

Decalcification of the previously fixed skull with the attached dura mater was performed using Osteosoft (Merck, Darmstadt, Germany) for 1 week at 4 °C, followed by sequential dehydration in 50%, 70%, 95%, and 100% ethanol and embedding in paraffin using an embedding station (Leica, Wetzlar, Germany). Ear samples were harvested and fixed in 4% PFA overnight at 4 °C, followed by sequential dehydration in 50%, 70%, 95%, and 100% ethanol, and embedding in paraffin. Eight-micrometer-thick sections were generated using a microtome (Thermo Fisher Scientific, HM340E, Waltham, USA) and immunostained with the following primary and secondary antibodies: anti-LYVE-1 (R&D Systems, AF2125, Minneapolis, USA), anti-PDPN (BioLegend, 127402, San Diego, USA), Alexa Fluor 488/568/594 anti-rabbit/anti-goat/anti-Syrian hamster IgG antibodies (Life Technologies, A21206, A11055, A11057, A11006, A11077, A21113, Waltham, USA) [32,35]. Nuclei were labeled with Vectashield DAPI Mounting Medium (Vector Laboratories, H-1200, Burlingame, USA).

2.8. Image acquisition and analysis

For microscopic imaging of histology slides, an upright microscope (Nikon Instruments, ECLIPSE Ni-U, Tokyo, Japan) with a 20 × dry objective connected to a camera (Nikon Instruments, DS-Ri2) was used. Whole-mount images were taken with a stereomicroscope (Nikon Instruments, SMZ-25) connected to a camera (Nikon Instruments, DS-Ri2), or a confocal microscope (Nikon Instruments, A1 HD25) using a 10x dry objective. For quantitative analysis of the dorsal meningeal lymphatics, stereomicroscopy images were used. Importantly, to quantify the meningeal lymphatics in the basal area (situated between the middle meningeal artery and the pterygopalatine artery), confocal imaging was required. Quantitative assessments including macromolecule drainage, length and area measurements were performed using NIS-Elements Imaging Software. Structure of the dorsal meningeal lymphatic vessels was characterized by two independent investigators blinded for all parameters (genotype, age, etc.) using a clinical score system on a scale from 0–15. The following parameters were assessed: continuity of meningeal lymphatic vessels; structural malformations of the meningeal lymphatics; presence of lymphatic vessels adjacent to the superior sagittal sinus, transverse sinus, and the middle meningeal arteries (dorsal region); and the number of branching points as previously described [33].

2.9. Presentation of data and statistical analysis

Experiments were performed the indicated number of times. For all experiments, investigators were blinded for the genotype of mice and treatment from the time of euthanasia to the end of the analysis. Quantitative graphs show mean ± SEM. Statistical analysis of data was performed using Graph Pad Prism 7.0 and Microsoft Office Excel software programs. Specific statistical tests for each experiment are indicated in the figure legends. *P*-values below 0.05 were considered statistically significant.

3. Results

3.1. CCBE1 reporter is expressed in the dura mater along the sinuses during the postnatal development of meningeal lymphatics

It has been well documented that meningeal lymphatics develop postnatally [30,33,36]. First, we characterized the developmental program of the meningeal lymphatic network by whole-mount immunostaining with anti-LYVE1 and anti-VWF antibodies to visualize lymphatic and blood endothelial markers. We found that meningeal lymphatic vessels were absent at P5 but well-developed lymphatics were detectable in young adult mice by P35 next to the transverse sinuses, sagittal sinuses, and basal area shown by stereo and confocal microscopy (Fig. 1A, D). The presence of the lymphatic structures was also quantified during the developmental period (Fig. 1B, C).

Next, we monitored the expression of CCBE1 during the postnatal developmental period using *Ccbe1*$^{LacZ/+}$ mice carrying a reporter allele and littermate controls. Importantly, we detected a robust CCBE1 reporter expression in the dura mater adjacent to sinuses before the presence of mature meningeal lymphatics at P7 and P15 compared to the *Ccbe1*$^{+/+}$ littermate controls (Fig. 2A and Suppl. Fig. 1). Notably, the expression levels of the CCBE1 reporter appeared to be stronger at the earlier time point. Histological analysis of the same samples was performed using anti-LYVE1 and anti-VWF antibodies. The VWF single positive blood vessels (confluence of sinuses) were apparent in the dura mater, but LYVE1 positive lymphatic vessels were not present at P7, while the formation of these lymphatic structures was detected by P15 (Fig. 2B). Importantly, blue precipitate was present in *Ccbe1*$^{LacZ/+}$ reporter mice in the dural layer next to the sinuses. We described the spatiotemporal changes of CCBE1 expression in the dural layers after birth indicating the strong expression of the marker adjacent to the venous sinuses alongside the developing lymphatic structures. These findings suggested that CCBE1 might be a regulator of the developmental program of meningeal lymphatics.

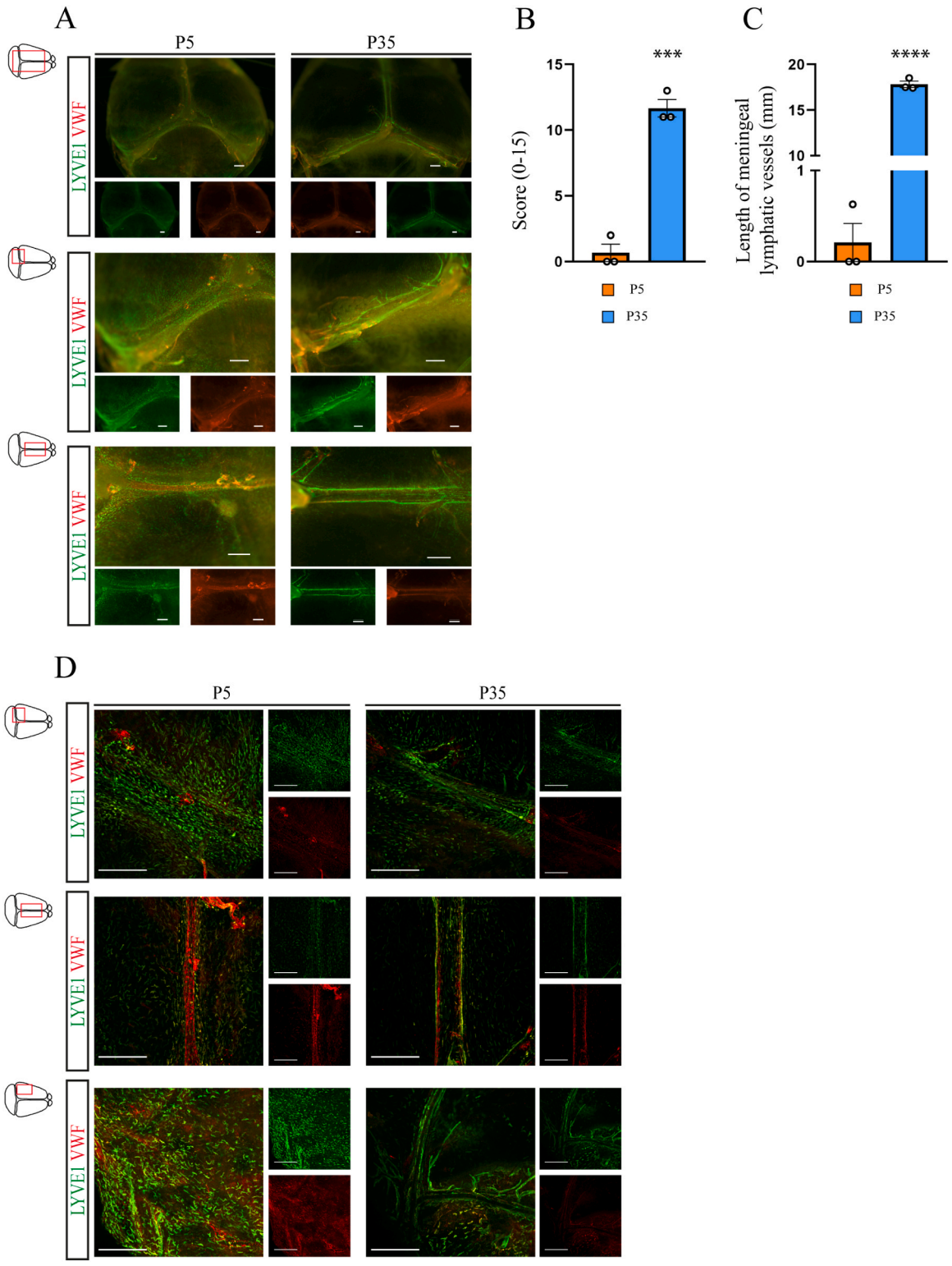

Fig. 1. Postnatal development of meningeal lymphatic vessels. A: LYVE1 and VWF whole-mount staining of the dural meninges adjacent to the transverse and the superior sagittal sinuses of newborn (P5) and young adult (P35) C57BL/6 wild type mice. Representative stereomicroscopy images are shown from n = 3 mice per group. Bars, 500 μm. **B, C:** Quantitative data are shown for clinical scores (0−15) representing structural integrity of the dorsal meningeal lymphatics (B) or length of the dorsal meningeal lymphatic vessels (mm) (C) of newborn mice (P5) and young adult (P35) C57BL/6 wild type mice. Data represented as mean ± SEM; unpaired two-tailed t-test; n = 3 mice per group; ***P < 0.001, ****P < 0.0001. **D:** LYVE1 and VWF whole-mount staining of the dural meninges adjacent to the transverse sinus, superior sagittal sinus, or middle meningeal artery (at the basal region) of newborn mice (P5) and young adult (P35) C57BL/6 wild type mice. Representative confocal (D) images are shown from n = 3 mice per group. Bars, 500 μm.

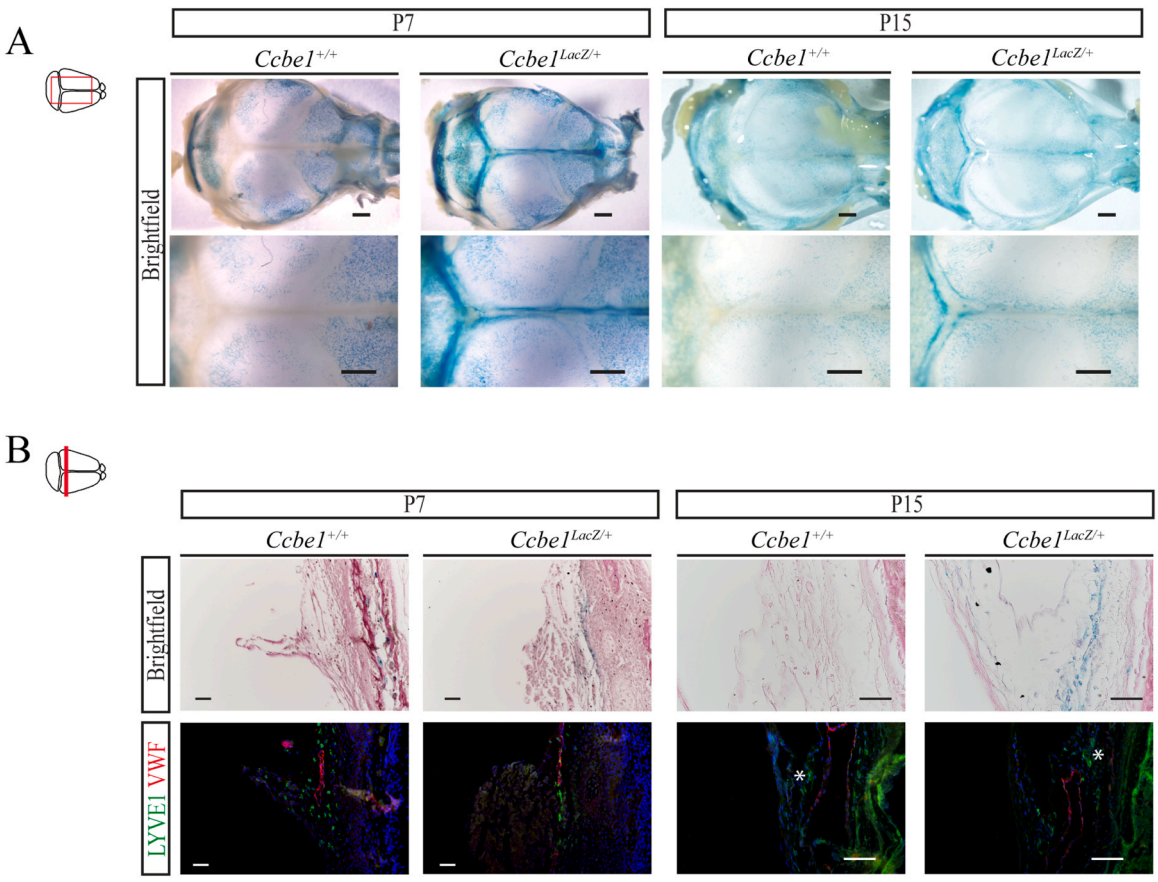

Fig. 2. CCBE1 reporter expression in the dura mater during the postnatal period. A: β-Gal whole-mount staining of the dural meninges of P7 and P15 wild type (*Ccbe1*$^{+/+}$) and *Ccbe1*$^{LacZ/+}$ reporter mice. Images were acquired by stereomicroscopy. Bars, 500 μm **B:** Cross-sections of the dural meninges of P7 and P15 wild type (*Ccbe1*$^{+/+}$) and *Ccbe1*$^{LacZ/+}$ mice, stained with β-Gal staining (upper panel) and immunofluorescence staining (lower panel) with antibodies against LYVE1 and VWF markers. White asterisks indicate the meningeal lymphatic vessels adjacent to the sinuses. Bars, 50 μm. Representative images of the experiments are shown; n = 3 mice per group.

3.2. CCBE1 is essential for the postnatal development of meningeal lymphatics

First, to test our conditional gene deletion strategy and to confirm prior findings showing the role of CCBE1 in lymphatic growth of the mouse skin [19], CCBE1 deletion was induced immediately after birth and lymphatic growth was monitored in the mouse ear, in an organ that develops postnatally (newborn mice have no ear formed), 45 days after birth. Lymphatic growth in the ear skin was greatly reduced in CCBE1-deleted mice compared to the littermate controls (Suppl. Fig. 2A, D). After quantification, the area and number of lymphatic vessels in the ear skin of CCBE1-deleted mice were significantly decreased in comparison to the control ears (Suppl. Fig. 2B, C).

Thereafter, we investigated the development of meningeal lymphatics after birth in mice with inducible deletion of *Ccbe1* at P0. To this end, deletion of the *Ccbe1* was induced in newborn mice at P0 in the Ub-CreER^{T2} system with intragastric Tamoxifen injection and in littermate controls, and the animals were sacrificed at P45. We found less meningeal lymphatics with altered structure along the transverse sinuses, sagittal sinuses, and the area of the basal skull in Ub-CreER^{T2}; *Ccbe1*$^{fl/-}$ mice by fluorescence stereomicroscopy 45 days after Tamoxifen treatment of newborns compared to the littermate controls (Fig. 3A). The evaluation of meningeal lymphatic vessels showed a decrease in score representing the structural integrity of meningeal lymphatics and the total length of the lymphatic network (Fig. 3B, C). Confocal imaging also indicated the great decrease of meningeal lymphatic structures in the dorsal region of Ub-CreER^{T2}; *Ccbe1*$^{fl/-}$ mice as well as in the basal region (Fig. 3D). Confocal imaging was used to quantify the dramatic decrease of meningeal lymphatics in the basal area (Fig. 3E). Of note, in the heterozygous mice (*Ccbe1*$^{fl/-}$ with no Cre expression), there is no significant difference in the presence of the meningeal structures compared to the wild type animals 45 days after birth (Suppl. Fig. 3A, B, C). Collectively, these findings indicate that CCBE1 acts as an important regulator in the organ-specific development of meningeal lymphatics.

3.3. Deletion of CCBE1 after birth reduces the lymphatic-mediated drainage of macromolecules

Next, we aimed to characterize the lymphatic-mediated macromolecule drainage from the CNS to the cervical region in mice with postnatal CCBE1 deletion immediately after birth. Labeled 70 kDa RhD was injected into the cisterna magna and brain parenchyma at 45 days after Tamoxifen treatment. The drainage of labeled macromolecules was assessed in the deep cervical lymph nodes of Ub-CreER^{T2}; *Ccbe1*$^{fl/-}$ mice and littermate controls. The accumulation of RhD in the deep cervical lymph nodes was greatly reduced in Ub-CreER^{T2}; *Ccbe1*$^{fl/-}$ mice after the cisterna magna and intraparenchymal injections (Fig. 4A, C). Quantification of the data indicates significantly impaired drainage to the deep cervical lymph nodes in Ub-CreER^{T2}; *Ccbe1*$^{fl/-}$ mice in comparison to the control mice (Fig. 4B, D). Confocal imaging revealed that absence of CCBE1 led to decreased macromolecule uptake into the meningeal lymphatic vessels after fluorescently labeled macromolecule injection (Fig. 4E). We also found accumulation of cells taking up RhD adjacent to the sinuses, especially in the CCBE1 deleted animals (Fig. 4E). These experiments indicate that impaired meningeal lymphatic development in animals with CCBE1 deletion at birth is associated with decreased

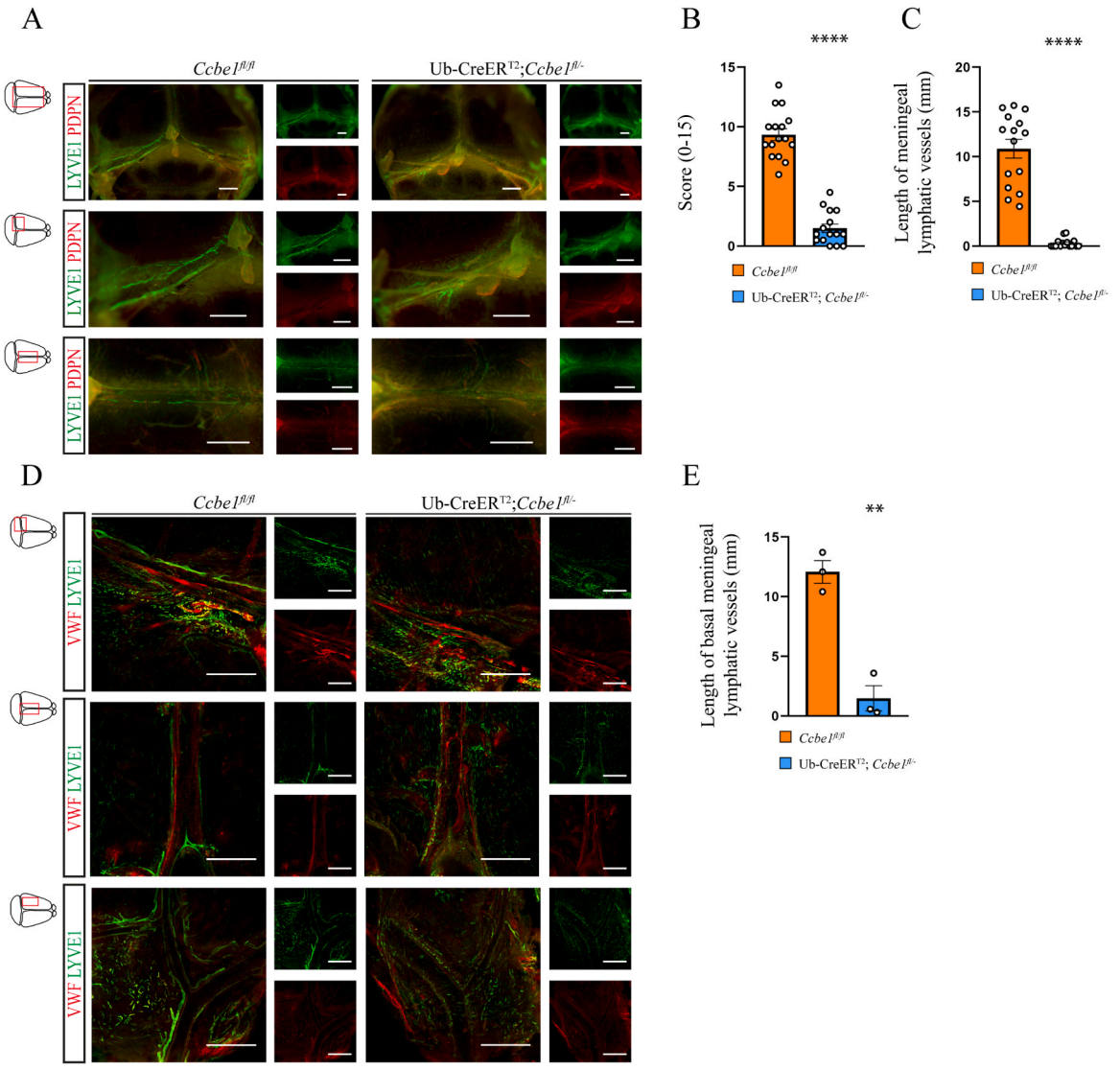

Fig. 3. Postnatal deletion of Ccbe1 prevents the development of meningeal lymphatic structures. A: LYVE1 and PDPN whole-mount staining of the dural meninges adjacent to transverse sinuses or the superior sagittal sinus of *Ccbe1*$^{fl/fl}$ and Ub-CreER^{T2}; *Ccbe1*$^{fl/-}$ mice 45 days post Tamoxifen treatment at P0. Representative fluorescence stereomicroscope images are shown from n = 3 mice per group. Bars, 1000 μm upper panel, 500 μm lower panel. **B, C:** Quantitative data are shown for clinical scores (0−15) representing structural malformations of the dorsal meningeal lymphatics (B) or length of the dorsal meningeal lymphatic vessels (mm) (C) in *Ccbe1*$^{fl/fl}$, and Ub-CreER^{T2}; *Ccbe1*$^{fl/-}$ mice 45 days post Tamoxifen treatment at P0. Data represented as mean ± SEM; unpaired two-tailed t-test (B) and Mann-Whitney U test (C); n = 15–16 mice per group; ****P < 0.0001. **D:** LYVE1 and VWF expression in the dural meninges adjacent to the transverse sinuses, superior sagittal sinus or at the basal region (next to middle meningeal artery and pterygopalatine artery) of *Ccbe1*$^{fl/fl}$ and Ub-CreER^{T2}; *Ccbe1*$^{fl/-}$ mice 45 days post Tamoxifen treatment at P0. Representative confocal images are shown from n = 3 mice per group. Bars, 500 μm. **E:** Quantitative data are shown for length of the basal meningeal lymphatic vessels (mm) representing structural malformations of the meningeal lymphatics in *Ccbe1*$^{fl/fl}$ and Ub-CreER^{T2}; *Ccbe1*$^{fl/-}$ mice 45 days post Tamoxifen treatment at P0. Data represented as mean ± SEM; unpaired two-tailed t-test; n = 3 mice per group; **P < 0.01.

macromolecular drainage from the CNS to the deep cervical lymph nodes.

3.4. *Meningeal lymphatic structures are altered by aging, mostly affecting the dorsal but not the basal meningeal compartments*

Although it has been described that meningeal lymphatics are altered by aging, most of these studies have focused on characterizing the dorsal region of the compartment in detail, we have only limited knowledge about the aging associated morphological changes of the basal area [4,28,29]. Therefore, we characterized the morphological changes of meningeal lymphatics by aging not only next to the transversal and sagittal sinuses but also in the basal area of the skull. Here we found a decrease in meningeal lymphatic vessel coverage in old (older than 18 months) mice in the dorsal region compared to adult (1–6 months) and middle-aged (10–14 months) animals (Fig. 5A; Suppl. Fig. 4A, B). Quantification of data showed a significant decrease in length and clinical score representing the integrity of the network of dorsal meningeal lymphatic vessels both in wild type and *Prox1*^{GFP} reporter mice (Fig. 5B, C; Suppl. Fig. 4C, D, E, F). In contrast, the basal meningeal lymphatic vessels did not show major signs of regression, instead they displayed structural alterations with a hyperplastic phenotype in aged mice compared to young mice in our experiments (Fig. 5D-G). Our results indicate that age-dependent alteration of meningeal lymphatic vessels mainly affects the dorsal region of the meningeal compartment.

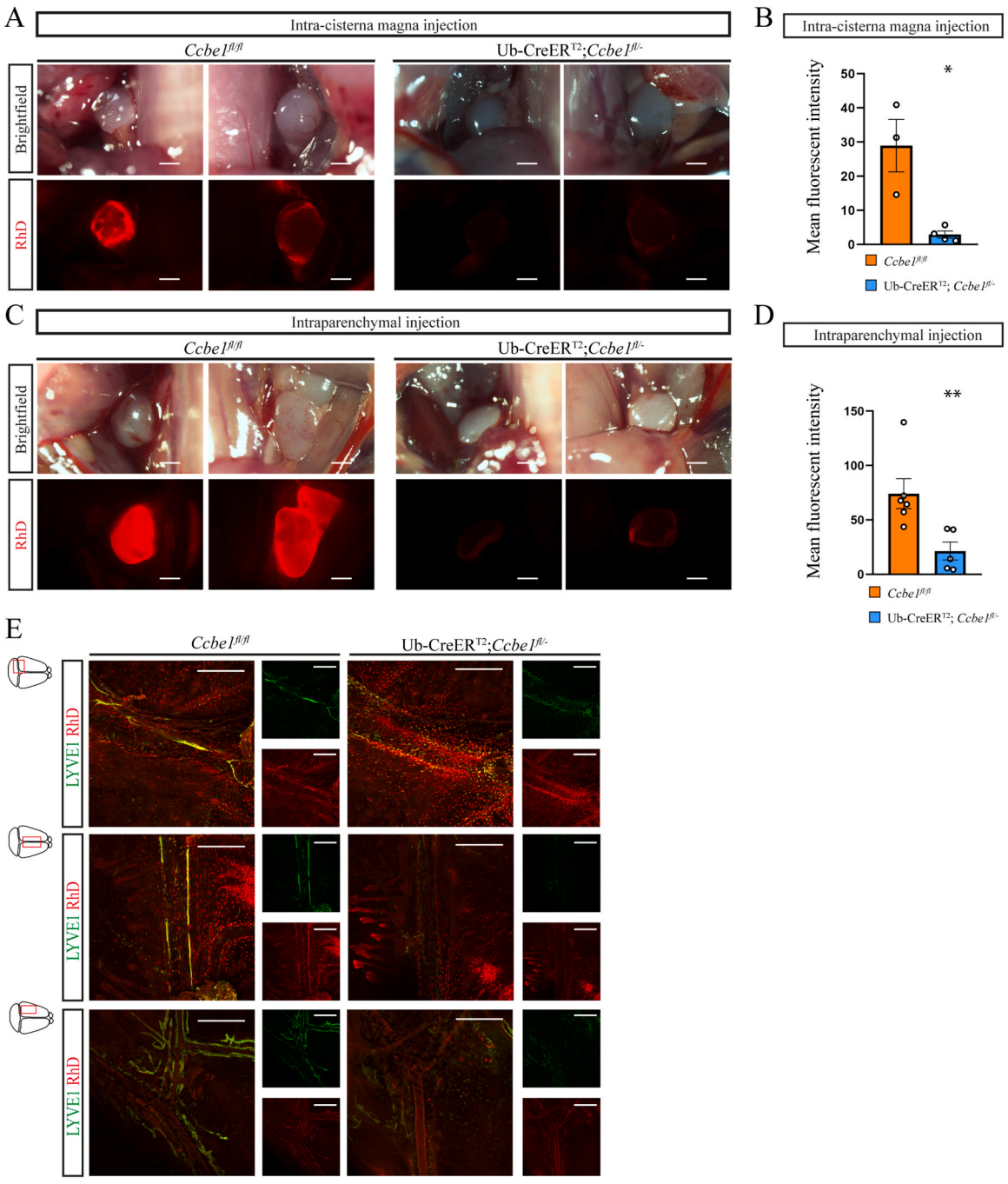

Fig. 4. Macromolecule drainage from the CNS after postnatal deletion of Ccbe1 after birth. A: Drainage of 70 kDa RhD into the deep cervical lymph nodes after injection of fluorescently labeled macromolecules into the cisterna magna of *Ccbe1*$^{fl/fl}$ and Ub-CreER^{T2}; *Ccbe1*$^{fl/-}$ mice 45 days post Tamoxifen treatment at P0. Representative fluorescence stereomicroscope images are shown from n = 3–4 mice per group. Bars, 500 μm. **B**: Quantitative data are shown for the mean fluorescence intensity in the deep cervical lymph nodes (mean fluorescence intensity of background subtracted from the mean fluorescence intensity of lymph nodes) after intra-cisterna magna **(A)** injection of 70 kDa RhD into *Ccbe1*$^{fl/fl}$ or Ub-CreER^{T2}; *Ccbe1*$^{fl/-}$ mice 45 days post Tamoxifen treatment at P0. Data represented as mean ± SEM; unpaired two-tailed t-test; n = 3–6 mice per group; *P < 0.05. **C**: Drainage of 70 kDa RhD into the deep cervical lymph nodes after injection of fluorescently labeled macromolecules into the brain parenchyma of *Ccbe1*$^{fl/fl}$ and Ub-CreER^{T2}; *Ccbe1*$^{fl/-}$ mice 45 days post Tamoxifen treatment at P0. Representative fluorescence stereomicroscope images are shown from n = 3–4 mice per group. Bars, 500 μm. **D**: Quantitative data are shown for the mean fluorescence intensity in the deep cervical lymph nodes (mean fluorescence intensity of background subtracted from the mean fluorescence intensity of lymph nodes) after into the brain parenchyma (**C**) injection of 70 kDa RhD into *Ccbe1*$^{fl/fl}$ or Ub-CreER^{T2}; *Ccbe1*$^{fl/-}$ mice 45 days post Tamoxifen treatment at P0. Data represented as mean ± SEM; Mann-Whitney U test; n = 3–6 mice per group; **P < 0.01. **E**: Representative confocal images shown for the RhD uptake by meningeal lymphatic vessels of transverse sinus, superior sagittal sinus and middle meningeal artery (at the basal region) 100 min after intraparenchymal injection of 70 kDa RhD into *Ccbe1*$^{fl/fl}$ and Ub-CreER^{T2}; *Ccbe1*$^{fl/-}$ mice 45 days post Tamoxifen treatment at P0. Representative images are shown from n = 3 mouse per group. Bars, 500 μm.

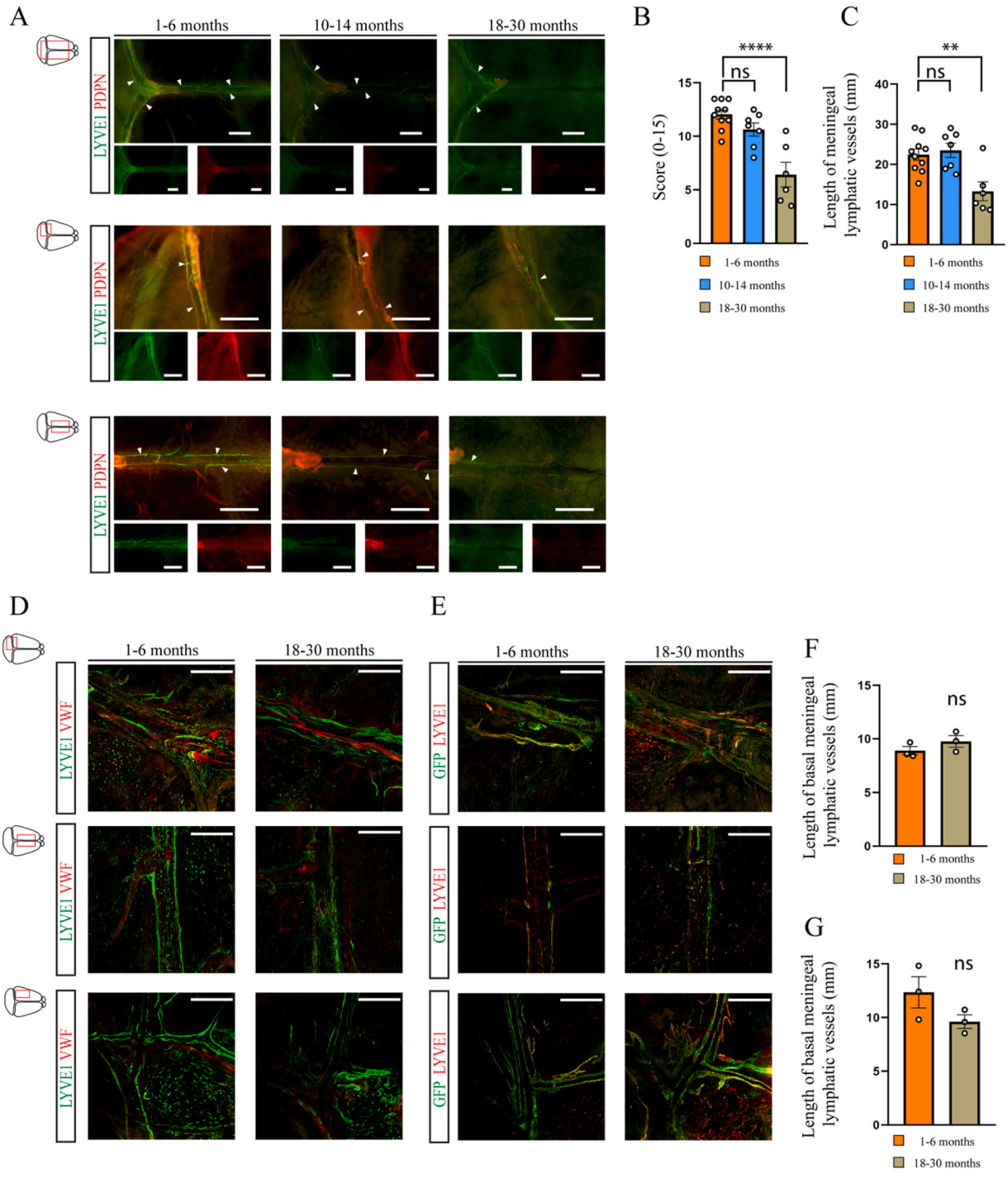

Fig. 5. Alterations of the meningeal lymphatic structures by aging. A: LYVE1 and PDPN whole-mount staining of the dural meninges adjacent to the transverse sinuses and superior sagittal sinus of adult (1–6 months old), middle-aged (10–14 months old) and old (18 or more months old) C57BL/6 wild type mice. Representative fluorescence stereomicroscope images are shown from n = 6–10 mice per group. White arrowheads indicate the meningeal lymphatic vessels adjacent to the sinuses. Bars, upper panel 1000 μm, lower panel 500 μm. **B, C:** Quantitative data are shown for clinical scores (0–15) representing structural malformations of the dorsal meningeal lymphatics (B) or length of the dorsal meningeal lymphatic vessels (mm) (C) in adult (1–6 months old), middle aged (10–14 months old) and old aged (18 or more months old) C57BL/6 wild type mice. Data represented as mean ± SEM; One-way ANOVA; Dunnett's post-hoc test, n = 6–10 mice per group, $^{**}P < 0.01$; $^{****}P < 0.0001$. **D:** LYVE1 and VWF whole-mount staining of the dural meninges adjacent to the transverse sinuses, superior sagittal sinus or middle meningeal artery (at the basal region) of adult (1–6 months old) and old aged (18 or more months old) C57BL/6 wild type mice. Representative confocal images are shown from n = 3 mice per group. Bars 500 μm. **E:** LYVE1 and GFP whole-mount staining of the dural meninges adjacent to the transverse sinuses, superior sagittal sinus or middle meningeal artery (at the basal region) of adult (1–6 months old) and old (18 or more months old) *Prox1*^{GFP} lymphatic reporter mice. Representative confocal images are shown from n = 3 mice per group. Bars 500 μm. **F:** Quantitative data are shown for length of the basal meningeal lymphatic vessels (mm) representing structural malformations of the meningeal lymphatics in adult (1–6 months old), and old aged (18 or more months old) C57BL/6 wild type mice. Data represented as mean ± SEM; unpaired two-tailed t-test; n = 3 mice per group; ns: not significant. **G**: Quantitative data are shown for length of the basal meningeal lymphatic vessels (mm) representing structural malformations of the meningeal lymphatics in adult (1–6 months old), and old (18 or more months old) *Prox1*^{GFP} lymphatic reporter mice. Data represented as mean ± SEM; unpaired two-tailed t-test; n = 3 mice per group, ns: not significant.

3.5. Deletion of CCBE1 in adults accelerates the age-dependent structural regression of meningeal lymphatic vessels

Meningeal lymphatics are fully developed by 35 days after birth (as shown in Fig. 1), and we found that meningeal lymphatics are not altered in young adult heterozygous mice at 45 days (Suppl. Fig. 3). Next, we characterized the role of CCBE1 in the maintenance of meningeal lymphatic vessels in adult animals. To this end, we induced the deletion of CCBE1 in 2-month-old animals, and assessed the lymphatic morphology and function at 3 months post deletion. We found regression of the meningeal lymphatic vessels not only in the dorsal but also in the basal region 3 months after the deletion of CCBE1 compared to control mice (Fig. 6A, D). The clinical score and total length representing the integrity of the lymphatic network of meningeal lymphatic vessels were significantly reduced compared to the littermate controls in Ub-CreER^{T2}; *Ccbe1*$^{fl/-}$ adult mice (Fig. 6B, C, E). Of note, no difference was detected in the presence and structure of blood vessels in the same animals. In older adult heterozygous mice (*Ccbe1*$^{fl/-}$ in the absence of the Cre expression), there was also some reduction in the presence of the meningeal structures compared to the wild type animals at 6–12 months of age (Suppl. Fig. 5), further suggesting the importance of CCBE1 levels (dosage) in the maintenance of meningeal lymphatic structures. In parallel, the morphology of ear lymphatics was characterized after CCBE1 deletion in adult animals. We performed the deletion of CCBE1 at 2 months of age and assessed the lymphatic morphology at 6 months post deletion by comparing it to the littermate controls. Importantly, no alterations were observed in the lymphatics of the ear skin in adult mice with Ub-CreER^{T2}; *Ccbe1*$^{fl/-}$ genotype (Suppl. Fig. 6). These results

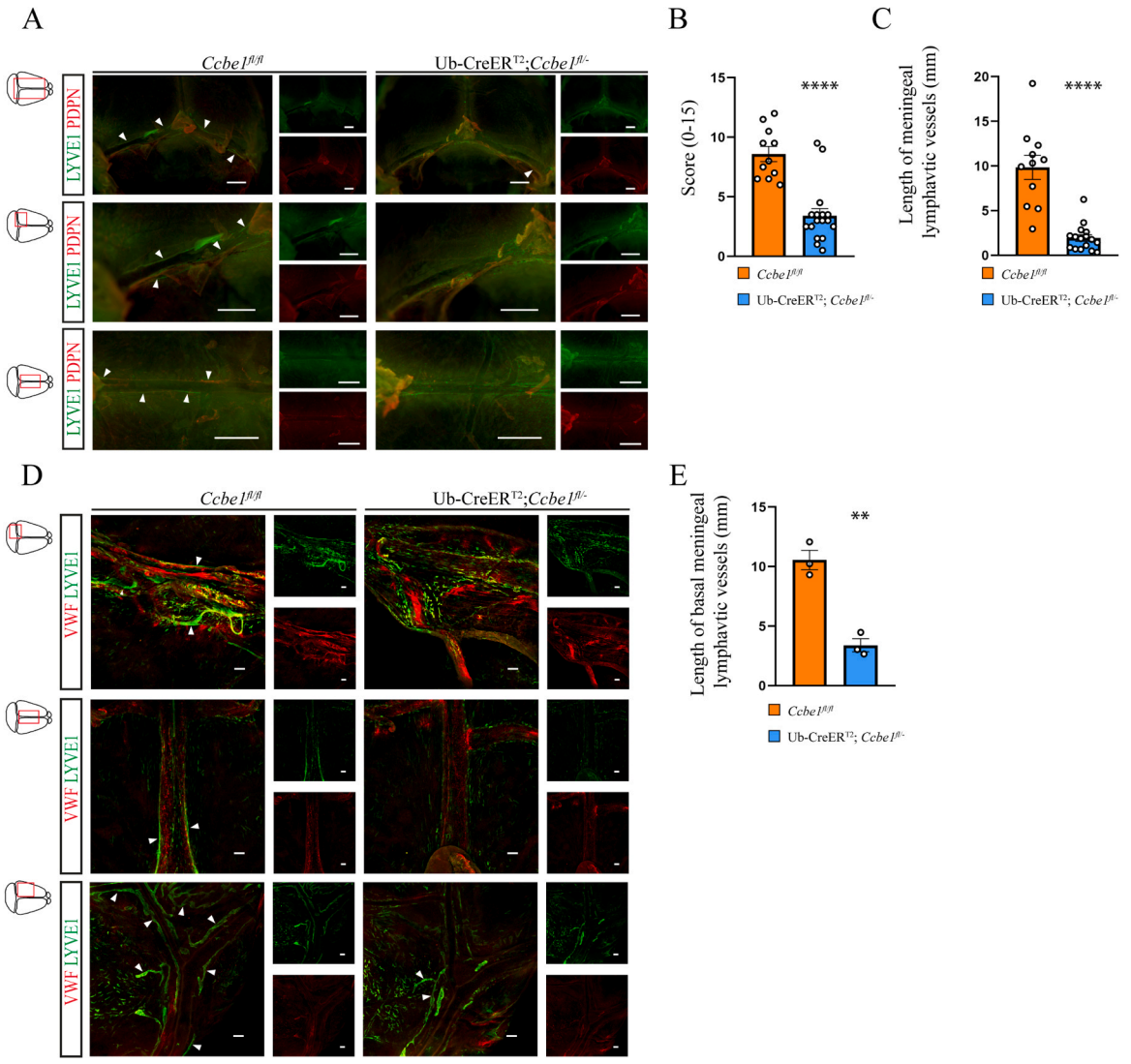

Fig. 6. Accelerated regression of meningeal lymphatics in adult Ccbe1-deleted mice. A: LYVE1 and PDPN whole-mount staining of the dural meninges adjacent to the transverse sinuses or superior sagittal sinus of *Ccbe1*$^{fl/fl}$ and Ub-CreER^{T2}; *Ccbe1*$^{fl/-}$ mice 3 months post Tamoxifen treatment of 2-month-old mice. Representative fluorescence stereomicroscope images are shown from n = 3 mice per group. White arrowheads indicate the meningeal lymphatic vessels adjacent to the sinuses. Bars, 1000 μm upper panel, 500 μm lower panels. **B, C:** Quantitative data are shown for clinical scores (0−15) representing structural malformations of the dorsal meningeal lymphatics (B) or length of the dorsal meningeal lymphatic vessels (mm) (C) in *Ccbe1*$^{fl/fl}$ and Ub-CreER^{T2}; *Ccbe1*$^{fl/-}$ mice 3 months post Tamoxifen treatment of 2-month-old mice. Data represented as mean ± SEM; Mann-Whitney U test; n = 11–17 mice per group; ****P < 0.0001. **D:** LYVE1 and VWF expression in the dural meninges and adjacent to the superior sagittal sinus, transverse sinuses or at the basal region of *Ccbe1*$^{fl/fl}$ and Ub-CreER^{T2}; *Ccbe1*$^{fl/-}$ mice 3 months post Tamoxifen treatment of 2-month-old mice. Representative confocal images are shown from n = 3 mice per group. White arrowheads indicate the meningeal lymphatic vessels adjacent to the sinuses. Bars, 100 μm. **E:** Quantitative data are shown for length of the basal meningeal lymphatic vessels (mm) representing structural malformations of the meningeal lymphatics in *Ccbe1*$^{fl/fl}$ and Ub-CreER^{T2}; *Ccbe1*$^{fl/-}$ mice 3 months post Tamoxifen treatment of 2-month-old mice. Data represented as Mean ± SEM; unpaired two-tailed t-test; n = 3 mice per group; **P < 0.01.

suggest an organ-specific importance of CCBE1 in the maintenance of meningeal lymphatic vessels.

3.6. The function of meningeal lymphatic vessels of CCBE1-deleted adult mice

To characterize the function of meningeal lymphatic vessels in Ub-CreER^{T2}; *Ccbe1*$^{fl/-}$ mice with the deletion during adulthood, we also monitored the RhD accumulation in deep cervical lymph nodes after CNS injections 3 months after the Cre induction at 2 months after birth. We found reduced labeled macromolecule accumulation in the deep cervical lymph nodes of Ub-CreER^{T2}; *Ccbe1*$^{fl/-}$ adult mice compared to the littermate controls, but the differences were not significant (Fig. 7 A-D). Importantly, there were fewer lymphatic vessels in the dorsal and basal region of Ub-CreER^{T2}; *Ccbe1*$^{fl/-}$ adult mice (Fig. 6E). Of note, the accumulation of RhD was detectable in the meningeal compartment with impaired meningeal lymphatic structures in Ub-CreER^{T2}; *Ccbe1*$^{fl/-}$ adult mice, especially next to the sinuses (Fig. 6E). In conclusion, the assessment of meningeal lymphatic vessels showed a significantly impaired morphology in mice with the adult deletion of CCBE1, and the drainage of macromolecules to the deep cervical lymph nodes was not significantly affected under our experimental conditions. These findings indicate that CCBE1 is needed for the normal maintenance of meningeal lymphatics in adult animals.

4. Discussion

In our studies, we have demonstrated that meningeal lymphatic structures develop during the postnatal period, in accordance with former publications [4,30,33,36]. Here, we also included the characterization of the developmental program of the lymphatic structures of the basal compartment in the dura mater (Fig. 1), which region has been implicated a critical functional role mediating the macromolecule drainage of the CNS [28].

The role of the VEGFC/VEGFR3 axis has already been described in the development of lymphatic vessels in various organs. The impaired VEGFC/VEGFR3 signaling pathway led to an arrest of the development and maturation of lymphatic vessels in the skin, intestine, and dura mater [30,37]. However, other organ-specific regulators that promote developmental lymphangiogenesis either by producing the mature and active form of VEGFC or through an independent signaling mechanism, are yet to be identified. Different molecules including ADAMTS3, CCBE1 and KLK3 were suggested being involved in the processing of VEGFC, mostly based on in vitro studies, and experiments focusing on the mouse skin, zebrafish models and spermatogenesis [17,18,38,39]. Here, we showed CCBE1 reporter expression in the dura mater after birth next to the sinuses, in parallel with the developmental process of meningeal lymphatics (Fig. 2). The histology samples show CCBE1 accumulation in cells adjacent to the VWF positive blood vessels and LYVE1 positive sprouting lymphatic vessels. Results in zebrafish suggest that CCBE1 is involved in the migration of lymphatic endothelial cells [40], and our finding raise the possibility a similar mechanism might be present in the meningeal compartment, but further studies are needed to characterize this process. A study suggested that lymphatic vessels draining the CNS are affected by the deletion of CCBE1 in zebrafish [41], but it is important to note that there are known differences in the molecular mechanisms in zebrafish and mouse models (e.g. Prox1 is dispensable for developmental lymphangiogenesis in zebrafish, while it is a critical factor in mice and humans) [42]. Therefore, we demonstrated in an inducible mouse model that CCBE1 has an organ-specific essential role in the development of meningeal lymphatics in different compartments of the dura mater (Fig. 3). Postnatal deletion of the CCBE1 arrested the developmental program of meningeal lymphatics affecting the dorsal region of the meningeal lymphatic vessels (next to the superior sagittal and transverse sinuses), and immature looking sprouting lymphatics were found at the basal region of the skull (Fig. 3). Impaired drainage of macromolecules from the CNS into the deep cervical lymph nodes mediated by meningeal lymphatics was also detected in the CCBE1-deleted young animals (Fig. 4). This impairment of lymphatic function was in accordance with the previous studies with the postnatal deletion of VEGFC lymphangiogenic factor where defective meningeal lymphatic development was associated with the decreased drainage of macromolecules to the deep cervical lymph nodes [30].

Age-dependent decline of lymphatic density and function has been described in the skin and the meningeal compartment, suggesting that alterations of organ-specific lymphatics function may be an important factor in the pathogenesis of aging-associated diseases [28,43,44]. In accordance, we found that the meningeal lymphatic structures in the dorsal region, particularly in vessels adjacent to superior sagittal sinus, are impaired in old mice (over 18 months) (Fig. 5), indicating that alteration of meningeal lymphatic vessels by aging mainly affects the dorsal region of the meningeal compartment. These results correlate with former studies describing that the initial meningeal lymphatic vessels are impaired by aging, and with those that reported malformation of the lymphatic structures in the basal region [4,28,29]. Further studies will be needed to better understand the age–related mechanisms involved in these regression processes.

In connection to the physiological regulators of the maintenance of meningeal lymphatics, we found a similar regressed pattern of meningeal lymphatic vessels in the dorsal region after the deletion of CCBE1 in adult mice to that present in aged wild type animals (Fig. 6). In addition, the inducible deletion of CCBE1 also affected the meningeal lymphatic vessels of the basal area (Fig. 6). Investigating the lymphatic function in CCBE1 deleted adult mice, we found a reduced tendency in the macromolecule drainage from the CNS (Fig. 7). It is possible that the presence of some remaining basal meningeal lymphatics or alternative draining routes may compensate the clearance of the macromolecules in CCBE1-deleted adult mice. Alternatively, our experimental setup for monitoring the drainage of macromolecules may not be sensitive enough for this adult functional model. Notably, both LYVE1-positive and non-positive cells adjacent to the sinuses were accumulated in the CCBE1-deleted adult mice, suggesting the impairment of the uptake and drainage of the macromolecules and cells (Fig. 7). Nevertheless, our results suggest that CCBE1-deleted mechanisms play an important role for the prevention of the age-related degeneration of meningeal lymphatics. In further experiments, the spatiotemporal expression pattern of CCBE1 should be investigated, which might have a different impact on the maintenance of meningeal lymphatics in various regions of the skull. Of note, no major alterations were present in the ear skin lymphatics in CCBE1-deleted adult mice indicating that CCBE1 has an organ-specific role in the meningeal compartment, where the protein showed a dosage-dependent role in the maintenance of lymphatic structures (Suppl. Fig. 6 and Fig. 6).

VEGFC/VEGFR3 signaling axis was reported to prevent the age-dependent regression of meningeal lymphatics, therefore the pathway is involved in the normal maintenance of these structures [30]. Further studies will be needed to reveal whether CCBE1 is important to support VEGFC/VEGFR3 signaling or is essential for an independent mechanism. Based on the prior in vitro cell culture-based, zebrafish and mouse skin studies focusing on developmental lymphangiogenesis the first possibility is the more likely scenario [17–19]. Importantly, our results suggest that CCBE1 is a potential therapeutic target to prevent the age-dependent regression of meningeal lymphatics, the structures which can be involved in the pathogenesis of diseases affecting the central nervous system (e.g., Alzheimer's disease, experimental autoimmune encephalomyelitis, etc.).

A recent study described another layer of the meninges, referred to as the subarachnoid lymphatic-like membrane (SLYM) [45]. The role of this structure raises many new questions in this field. It would be interesting to explore the effects of CCBE1 deficiency, for instance, on this extra layer, and to understand the distribution of the clearance between the meningeal lymphatic vessels and SLYM. In the future, it will

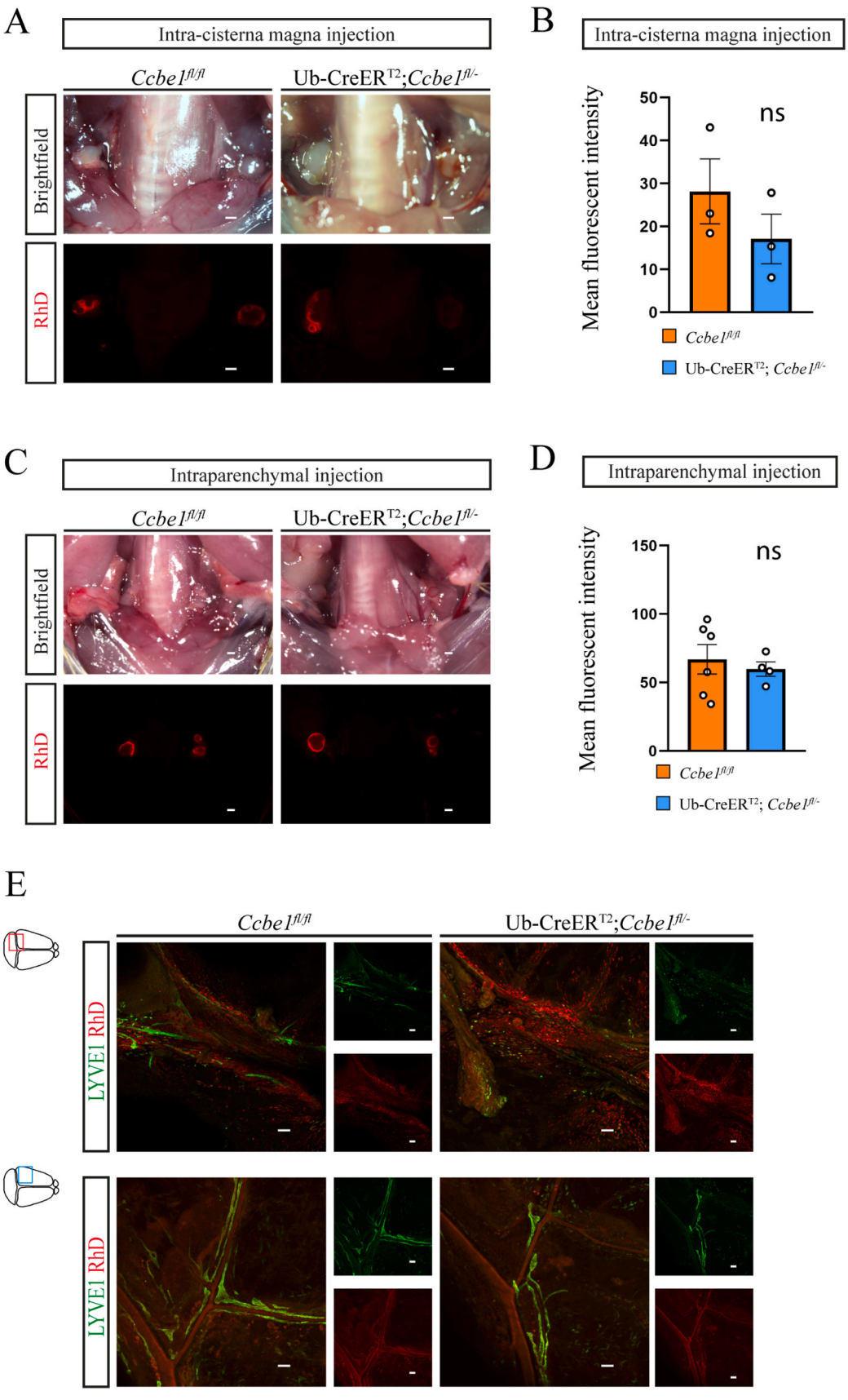

(caption on next page)

Fig. 7. Macromolecule drainage from the CNS after conditional deletion of Ccbe1 in adult mice. **A**: Drainage of fluorescently labeled macromolecules into the deep cervical lymph nodes 100 min after the injection of 70 kDa RhD into the cisterna magna of *Ccbe1*$^{fl/fl}$ and Ub-CreER^{T2}; *Ccbe1*$^{fl/-}$ mice 3 months post Tamoxifen treatment of 2-month-old mice. Representative fluorescence stereomicroscope images are shown from n = 3 mice per group. Bars, 500 μm. **B**: Quantitative data are shown for mean fluorescence intensity in the deep cervical lymph nodes (mean fluorescence intensity of background subtracted from the mean fluorescence intensity of lymph nodes) after intra-cisterna magna **(A)** injection of 70 kDa RhD into *Ccbe1*$^{fl/fl}$ and Ub-CreER^{T2}; *Ccbe1*$^{fl/-}$ mice 3 months post Tamoxifen treatment of 2-month-old mice. Data represented as mean ± SEM; unpaired two-tailed t-test; n = 3 mice per group. **C**: Drainage of fluorescently labeled macromolecules into the deep cervical lymph nodes 100 min after the injection of 70 kDa RhD into the brain parenchyma of *Ccbe1*$^{fl/fl}$ and Ub-CreER^{T2}; *Ccbe1*$^{fl/-}$ mice 3 months post Tamoxifen treatment of 2-month-old mice. Representative fluorescence stereomicroscope images are shown from n = 4–6 mice per group. Bars, 500 μm. **D**: Quantitative data are shown for mean fluorescence intensity in the deep cervical lymph nodes (mean fluorescence intensity of background subtracted from the mean fluorescent intensity of lymph nodes) after intraparenchymal **(C)** injection of 70 kDa RhD into *Ccbe1*$^{fl/fl}$ and Ub-CreER^{T2}; *Ccbe1*$^{fl/-}$ mice 3 months post Tamoxifen treatment of 2-month-old mice. Data represented as mean ± SEM; unpaired two-tailed t-test; n = 4–6 mice per group. **E**: RhD uptake by meningeal lymphatic vessels adjacent to the transverse sinuses and middle meningeal artery (at the basal region) 100 min after intraparenchymal injection of 70 kDa RhD of *Ccbe1*$^{fl/fl}$ and Ub-CreER^{T2}; *Ccbe1*$^{fl/-}$ mice 3 months post Tamoxifen treatment of 2-month-old mice. Representative images are shown from n = 3 mouse per group. Bars, 100 μm.

be of great importance to characterize these connections in detail.

Taken together, our results indicate the importance of CCBE1-dependent mechanisms not only in the development, but also in the prevention of the age-related regression of meningeal lymphatics. Therefore, targeting CCBE1 may be a good therapeutic strategy to prevent age-related degeneration of meningeal lymphatics.

Ethics approval

All animal experiments were approved by the Animal Experimentation Review Board of the Semmelweis University and the Government Office for Pest County (Hungary).

Funding

This work was supported by the National Research, Development and Innovation Office (K139165, TKP2021-EGA-29, TKP2021-EGA-24, NVKP_16-1-2016-0039), the European Union and the Hungarian Government (VEKOP-2.3.2–16-2016-00002, VEKOP-2.3.3-15-2016-00006, EFOP-3.6.3-VEKOP-16–2017-00009). Z.J. is a recipient of the János Bolyai Research Scholarship of the Hungarian Academy of Sciences (BO/00898/22) and the New National Excellence Program of the Ministry for Culture and Innovation from the source of the National Research, Development and Innovation Fund (UNKP-23-5-SE-10).

CRediT authorship contribution statement

Zsombor Ocskay: Conceptualization, Investigation, Methodology, Formal analysis, Visualization, Writing – original draft. **Laszlo Balint:** Investigation, Methodology, Formal analysis, Writing – review & editing. **Carolin Christ:** Investigation, Formal analysis, Writing – review & editing. **Mark L. Kahn:** Methodology, Writing – review & editing. **Zoltan Jakus:** Conceptualization, Investigation, Methodology, Formal analysis, Writing – original draft, Supervision, Project administration, Funding acquisition.

Declaration of Competing Interest

The authors declare that they have no known competing financial interests or personal relationships that could have appeared to influence the work reported in this paper.

Data Availability

Data will be made available on request.

Acknowledgements

We thank V. Németh, E. Marinkás, Á. Marinkás and D. Csengel for excellent technical assistance and Young-Kwon Hong for the *Prox1*^{GFP} mice.

Authorship contribution

Zs.O. and Z.J. designed the work, interpreted the results and wrote the paper. Zs.O., L.B., C.C., and Z.J. performed the experiments, analyzed the data, and reviewed and edited the manuscript. M.L.K. provided genetic models for the inducible deletion of CCBE1 and reviewed the manuscript. Z. J. supervised the project.

Appendix A. Supporting information

Supplementary data associated with this article can be found in the online version at doi:10.1016/j.biopha.2023.116032.

References

[1] A. Aspelund, M.R. Robciuc, S. Karaman, T. Makinen, K. Alitalo, Lymphatic system in cardiovascular medicine, Circ. Res 118 (3) (2016) 515–530.
[2] G. Oliver, J. Kipnis, G.J. Randolph, N.L. Harvey, The lymphatic vasculature in the 21(st) century: novel functional roles in homeostasis and disease, Cell 182 (2) (2020) 270–296.
[3] A. Aspelund, S. Antila, S.T. Proulx, T.V. Karlsen, S. Karaman, M. Detmar, H. Wiig, K. Alitalo, A dural lymphatic vascular system that drains brain interstitial fluid and macromolecules, J. Exp. Med 212 (7) (2015) 991–999.
[4] S. Da Mesquita, Z. Fu, J. Kipnis, The meningeal lymphatic system: a new player in neurophysiology, Neuron 100 (2) (2018) 375–388.
[5] M.J. Karkkainen, P. Haiko, K. Sainio, J. Partanen, J. Taipale, T.V. Petrova, M. Jeltsch, D.G. Jackson, M. Talikka, H. Rauvala, C. Betsholtz, K. Alitalo, Vascular endothelial growth factor C is required for sprouting of the first lymphatic vessels from embryonic veins, Nat. Immunol. 5 (1) (2004) 74–80.
[6] V. Joukov, K. Pajusola, A. Kaipainen, D. Chilov, I. Lahtinen, E. Kukk, O. Saksela, N. Kalkkinen, K. Alitalo, A novel vascular endothelial growth factor, VEGF-C, is a ligand for the Flt4 (VEGFR-3) and KDR (VEGFR-2) receptor tyrosine kinases, EMBO J. 15 (2) (1996) 290–298.
[7] S.J. Oh, M.M. Jeltsch, R. Birkenhager, J.E. McCarthy, H.A. Weich, B. Christ, K. Alitalo, J. Wilting, VEGF and VEGF-C: specific induction of angiogenesis and lymphangiogenesis in the differentiated avian chorioallantoic membrane, Dev. Biol. 188 (1) (1997) 96–109.
[8] M. Jeltsch, A. Kaipainen, V. Joukov, X. Meng, M. Lakso, H. Rauvala, M. Swartz, D. Fukumura, R.K. Jain, K. Alitalo, Hyperplasia of lymphatic vessels in VEGF-C transgenic mice, Science 276 (5317) (1997) 1423–1425.
[9] M.J. Karkkainen, R.E. Ferrell, E.C. Lawrence, M.A. Kimak, K.L. Levinson, M. A. McTigue, K. Alitalo, D.N. Finegold, Missense mutations interfere with VEGFR-3 signalling in primary lymphoedema, Nat. Genet 25 (2) (2000) 153–159.
[10] I.D. Van Balkom, M. Alders, J. Allanson, C. Bellini, U. Frank, G. De Jong, I. Kolbe, D. Lacombe, S. Rockson, P. Rowe, F. Wijburg, R.C. Hennekam, Lymphedema-lymphangiectasia-mental retardation (Hennekam) syndrome: a review, Am. J. Med Genet 112 (4) (2002) 412–421.
[11] M. Alders, B.M. Hogan, E. Gjini, F. Salehi, L. Al-Gazali, E.A. Hennekam, E. E. Holmberg, M.M. Mannens, M.F. Mulder, G.J. Offerhaus, T.E. Prescott, E. J. Schroor, J.B. Verheij, M. Witte, P.J. Zwijnenburg, M. Vikkula, S. Schulte-Merker, R.C. Hennekam, Mutations in CCBE1 cause generalized lymph vessel dysplasia in humans, Nat. Genet 41 (12) (2009) 1272–1274.
[12] M. Alders, A. Mendola, L. Ades, L. Al Gazali, C. Bellini, B. Dallapiccola, P. Edery, U. Frank, F. Hornshuh, S.A. Huisman, S. Jagadeesh, H. Kayserili, W.T. Keng, D. Lev, C.E. Prada, J.R. Sampson, J. Schmidtke, V. Shashi, Y. van Bever, N. Van der Aa, J. M. Verhagen, J.B. Verheij, M. Vikkula, R.C. Hennekam, Evaluation of clinical manifestations in patients with severe lymphedema with and without CCBE1 mutations, Mol. Syndr. 4 (3) (2013) 107–113.
[13] B.M. Hogan, F.L. Bos, J. Bussmann, M. Witte, N.C. Chi, H.J. Duckers, S. Schulte-Merker, Ccbe1 is required for embryonic lymphangiogenesis and venous sprouting, Nat. Genet 41 (4) (2009) 396–398.
[14] F.L. Bos, M. Caunt, J. Peterson-Maduro, L. Planas-Paz, J. Kowalski, T. Karpanen, A. van Impel, R. Tong, J.A. Ernst, J. Korving, J.H. van Es, E. Lammert, H. J. Duckers, S. Schulte-Merker, CCBE1 is essential for mammalian lymphatic

vascular development and enhances the lymphangiogenic effect of vascular endothelial growth factor-C in vivo, Circ. Res 109 (5) (2011) 486–491.
[15] Z. Zou, D.R. Enis, H. Bui, E. Khandros, V. Kumar, Z. Jakus, C. Thom, Y. Yang, V. Dhillon, M. Chen, M. Lu, M.J. Weiss, M.L. Kahn, The secreted lymphangiogenic factor CCBE1 is essential for fetal liver erythropoiesis, Blood 121 (16) (2013) 3228–3236.
[16] R. Hagerling, C. Pollmann, M. Andreas, C. Schmidt, H. Nurmi, R.H. Adams, K. Alitalo, V. Andresen, S. Schulte-Merker, F. Kiefer, A novel multistep mechanism for initial lymphangiogenesis in mouse embryos based on ultramicroscopy, EMBO J. 32 (5) (2013) 629–644.
[17] M. Jeltsch, S.K. Jha, D. Tvorogov, A. Anisimov, V.M. Leppanen, T. Holopainen, R. Kivela, S. Ortega, T. Karpanen, K. Alitalo, CCBE1 enhances lymphangiogenesis via A disintegrin and metalloprotease with thrombospondin motifs-3-mediated vascular endothelial growth factor-C activation, Circulation 129 (19) (2014) 1962–1971.
[18] L. Le Guen, T. Karpanen, D. Schulte, N.C. Harris, K. Koltowska, G. Roukens, N. I. Bower, A. van Impel, S.A. Stacker, M.G. Achen, S. Schulte-Merker, B.M. Hogan, Ccbe1 regulates Vegfc-mediated induction of Vegfr3 signaling during embryonic lymphangiogenesis, Development 141 (6) (2014) 1239–1249.
[19] H.M. Bui, D. Enis, M.R. Robciuc, H.J. Nurmi, J. Cohen, M. Chen, Y. Yang, V. Dhillon, K. Johnson, H. Zhang, R. Kirkpatrick, E. Traxler, A. Anisimov, K. Alitalo, M.L. Kahn, Proteolytic activation defines distinct lymphangiogenic mechanisms for VEGFC and VEGFD, J. Clin. Invest 126 (6) (2016) 2167–2180.
[20] A. Louveau, I. Smirnov, T.J. Keyes, J.D. Eccles, S.J. Rouhani, J.D. Peske, N. C. Derecki, D. Castle, J.W. Mandell, K.S. Lee, T.H. Harris, J. Kipnis, Structural and functional features of central nervous system lymphatic vessels, Nature 523 (7560) (2015) 337–341.
[21] S. Gonzalez-Hernandez, Y.S. Mukouyama, Lymphatic vasculature in the central nervous system, Front Cell Dev. Biol. 11 (2023) 1150775.
[22] G. Castellani, T. Croese, J.M. Peralta Ramos, M. Schwartz, Transforming the understanding of brain immunity, Science 380 (6640) (2023), eabo7649.
[23] M. Absinta, S.K. Ha, G. Nair, P. Sati, N.J. Luciano, M. Palisoc, A. Louveau, K. A. Zaghloul, S. Pittaluga, J. Kipnis, D.S. Reich, Human and nonhuman primate meninges harbor lymphatic vessels that can be visualized noninvasively by MRI, Elife 6 (2017).
[24] A. Louveau, J. Herz, M.N. Alme, A.F. Salvador, M.Q. Dong, K.E. Viar, S.G. Herod, J. Knopp, J.C. Setliff, A.L. Lupi, S. Da Mesquita, E.L. Frost, A. Gaultier, T.H. Harris, R. Cao, S. Hu, J.R. Lukens, I. Smirnov, C.C. Overall, G. Oliver, J. Kipnis, CNS lymphatic drainage and neuroinflammation are regulated by meningeal lymphatic vasculature, Nat. Neurosci. 21 (10) (2018) 1380–1391.
[25] S. Da Mesquita, A. Louveau, A. Vaccari, I. Smirnov, R.C. Cornelison, K. M. Kingsmore, C. Contarino, S. Onengut-Gumuscu, E. Farber, D. Raper, K.E. Viar, R.D. Powell, W. Baker, N. Dabhi, R. Bai, R. Cao, S. Hu, S.S. Rich, J.M. Munson, M. B. Lopes, C.C. Overall, S.T. Acton, J. Kipnis, Functional aspects of meningeal lymphatics in ageing and Alzheimer's disease, Nature 560 (7717) (2018) 185–191.
[26] M. Hsu, A. Rayasam, J.A. Kijak, Y.H. Choi, J.S. Harding, S.A. Marcus, W.J. Karpus, M. Sandor, Z. Fabry, Neuroinflammation-induced lymphangiogenesis near the cribriform plate contributes to drainage of CNS-derived antigens and immune cells, Nat. Commun. 10 (1) (2019), 229.
[27] T.K. Patel, L. Habimana-Griffin, X. Gao, B. Xu, S. Achilefu, K. Alitalo, C.A. McKee, P.W. Sheehan, E.S. Musiek, C. Xiong, D. Coble, D.M. Holtzman, Dural lymphatics regulate clearance of extracellular tau from the CNS, Mol. Neurodegener. 14 (1) (2019), 11.
[28] J.H. Ahn, H. Cho, J.H. Kim, S.H. Kim, J.S. Ham, I. Park, S.H. Suh, S.P. Hong, J. H. Song, Y.K. Hong, Y. Jeong, S.H. Park, G.Y. Koh, Meningeal lymphatic vessels at the skull base drain cerebrospinal fluid, Nature 572 (7767) (2019) 62–66.
[29] Y. Zhou, J. Cai, W. Zhang, X. Gong, S. Yan, K. Zhang, Z. Luo, J. Sun, Q. Jiang, M. Lou, Impairment of the glymphatic pathway and putative meningeal lymphatic vessels in the aging human, Ann. Neurol. 87 (3) (2020) 357–369.
[30] S. Antila, S. Karaman, H. Nurmi, M. Airavaara, M.H. Voutilainen, T. Mathivet, D. Chilov, Z. Li, T. Koppinen, J.H. Park, S. Fang, A. Aspelund, M. Saarma, A. Eichmann, J.L. Thomas, K. Alitalo, Development and plasticity of meningeal lymphatic vessels, J. Exp. Med 214 (12) (2017) 3645–3667.
[31] I. Choi, H.K. Chung, S. Ramu, H.N. Lee, K.E. Kim, S. Lee, J. Yoo, D. Choi, Y.S. Lee, B. Aguilar, Y.K. Hong, Visualization of lymphatic vessels by Prox1-promoter directed GFP reporter in a bacterial artificial chromosome-based transgenic mouse, Blood 117 (1) (2011) 362–365.
[32] Z. Jakus, J.P. Gleghorn, D.R. Enis, A. Sen, S. Chia, X. Liu, D.R. Rawnsley, Y. Yang, P.R. Hess, Z. Zou, J. Yang, S.H. Guttentag, C.M. Nelson, M.L. Kahn, Lymphatic function is required prenatally for lung inflation at birth, J. Exp. Med 211 (5) (2014) 815–826.
[33] L. Balint, Z. Ocskay, B.A. Deak, P. Aradi, Z. Jakus, Lymph flow induces the postnatal formation of mature and functional meningeal lymphatic vessels, Front Immunol. 10 (2019) 3043.
[34] M.C. Puri, J. Rossant, K. Alitalo, A. Bernstein, J. Partanen, The receptor tyrosine kinase TIE is required for integrity and survival of vascular endothelial cells, EMBO J. 14 (23) (1995) 5884–5891.
[35] D. Szoke, G. Kovacs, E. Kemecsei, L. Balint, K. Szotak-Ajtay, P. Aradi, A. Styevkone Dinnyes, B.L. Mui, Y.K. Tam, T.D. Madden, K. Kariko, R.P. Kataru, M.J. Hope, D. Weissman, B.J. Mehrara, N. Pardi, Z. Jakus, Nucleoside-modified VEGFC mRNA induces organ-specific lymphatic growth and reverses experimental lymphedema, Nat. Commun. 12 (1) (2021), 3460.
[36] R.M. Izen, T. Yamazaki, Y. Nishinaka-Arai, Y.K. Hong, Y.S. Mukouyama, Postnatal development of lymphatic vasculature in the brain meninges, Dev. Dyn. 247 (5) (2018) 741–753.
[37] H. Nurmi, P. Saharinen, G. Zarkada, W. Zheng, M.R. Robciuc, K. Alitalo, VEGF-C is required for intestinal lymphatic vessel maintenance and lipid absorption, EMBO Mol. Med 7 (11) (2015) 1418–1425.
[38] S.K. Jha, K. Rauniyar, T. Karpanen, V.M. Leppanen, P. Brouillard, M. Vikkula, K. Alitalo, M. Jeltsch, Efficient activation of the lymphangiogenic growth factor VEGF-C requires the C-terminal domain of VEGF-C and the N-terminal domain of CCBE1, Sci. Rep. 7 (1) (2017), 4916.
[39] S.K. Jha, K. Rauniyar, E. Chronowska, K. Mattonet, E.W. Maina, H. Koistinen, U. H. Stenman, K. Alitalo, M. Jeltsch, KLK3/PSA and cathepsin D activate VEGF-C and EGF-D, Elife 8 (2019).
[40] G. Wang, L. Muhl, Y. Padberg, L. Dupont, J. Peterson-Maduro, M. Stehling, F. le Noble, A. Colige, C. Betsholtz, S. Schulte-Merker, A. van Impel, Specific fibroblast subpopulations and neuronal structures provide local sources of Vegfc-processing components during zebrafish lymphangiogenesis, Nat. Commun. 11 (1) (2020), 2724.
[41] M. van Lessen, S. Shibata-Germanos, A. van Impel, T.A. Hawkins, J. Rihel, S. Schulte-Merker, Intracellular uptake of macromolecules by brain lymphatic endothelial cells during zebrafish embryonic development, Elife 6 (2017).
[42] A. van Impel, Z. Zhao, D.M. Hermkens, M.G. Roukens, J.C. Fischer, J. Peterson-Maduro, H. Duckers, E.A. Ober, P.W. Ingham, S. Schulte-Merker, Divergence of zebrafish and mouse lymphatic cell fate specification pathways, Development 141 (6) (2014) 1228–1238.
[43] S. Karaman, D. Buschle, P. Luciani, J.C. Leroux, M. Detmar, S.T. Proulx, Decline of lymphatic vessel density and function in murine skin during aging, Angiogenesis 18 (4) (2015) 489–498.
[44] R.P. Kataru, H.J. Park, J. Shin, J.E. Baik, A. Sarker, S. Brown, B.J. Mehrara, Structural and functional changes in aged skin lymphatic vessels, Front. Aging 3 (2022), 864860.
[45] K. Mollgard, F.R.M. Beinlich, P. Kusk, L.M. Miyakoshi, C. Delle, V. Pla, N. L. Hauglund, T. Esmail, M.K. Rasmussen, R.S. Gomolka, Y. Mori, M. Nedergaard, A mesothelium divides the subarachnoid space into functional compartments, Science 379 (6627) (2023) 84–88.